ELSEVIER

S0032-3861(96)00436-3

Polymer Vol. 37 No. 25, pp. 5715–5725, 1996

0032-3861/96/$15.00 + 0.00

Chemically induced phase separation: a new technique for the synthesis of macroporous epoxy networks

J. Kiefer and J. G. Hilborn*
Swiss Federal Institute of Technology, Materials Department, Polymers Laboratory, CH-1015 Lausanne, Switzerland

and J. L. Hedrick
IBM Research Division, Almaden Research Center, 650 Harry Road, San Jose, CA 95120-6099, USA
(Received 5 February 1996; revised 1 April 1996)

We have developed a new technology, based on chemically induced phase separation, that allows for the synthesis of porous epoxies with a closed cell morphology and a narrow pore size distribution in the micrometre range. The potential of this technique for the synthesis of new types of porous thermosets is enlightened by the comparison with the current state of the art on technologies for the preparation of macroporous polymeric materials. The strategy of the chemically induced phase separation technique, as a general approach for the synthesis of macroporous thermosets with controlled morphology is presented. The particular system reported is a diglycidylether of bisphenol-A cured with 2,2′-bis(4-amino-cyclohexyl)-propane in the presence of hexane or cyclohexane. Depending on the hexane concentration, the morphology can be varied ranging from a monomodal to bimodal distribution. By regarding the kinetics and the development of a bimodal distribution, we surmise that the phase separation proceeds via a nucleation and growth mechanism. The influence of internal and external reaction parameters, such as chemical nature of the solvent, solvent concentration and curing temperature on the final morphology are reported. These porous materials are characterized by a significantly lower density without any loss in thermal stability compared to the neat matrix. Copyright © 1996 Elsevier Science Ltd.

(Keywords: macroporous epoxies; chemically induced phase separation; nucleation and growth)

INTRODUCTION

Porous polymers have found use for numerous applications such as foams, membranes, filters, chromatography media, and solid support. These materials have many useful properties including low density, good thermal and electric isolation, and high specific surface. The key feature in their preparation is the control of porosity leading to either open or closed cell structures of various size and size distribution.

According to a nomenclature proposed by IUPAC, porous materials with pore sizes greater than 50 nm should be termed macroporous[1]. Based on this terminology, porous materials with pore diameters lower than 2 nm should be called microporous. The nomination mesoporous is reserved for porous materials with intermediate pore sizes.

The techniques for the preparation of porous polymers can be classified into three main types.

Firstly, blowing is the most common method to produce macroporous foams. The blowing agent may either be mixed in or be produced in an exothermic crosslinking reaction[2]. For example, flexible polyurethane foams are commercially produced using carbon dioxide, which is generated through the reaction of the isocyanate with water. Owing to the high diffusion rate of gases in polymers, this technique yields foams with a large pore size distribution ranging over several orders of magnitude. Very recently polymeric foams with a bimodal pore size distribution have been reported, which exhibit a considerable improvement in compressive strength[3]. The generation of such a bimodal pore size distribution requires a thermal shock and the use of nucleation agents for morphology control.

Alternatively blowing can be done by a gas nucleation technique used since the early eighties for the preparation of microcelluar thermoplastic foams, such as PP, PS, PC, PVC, PET or ABS, with bubble densities up to 10^9 cells cm^{-3} [4,5]. This method consists of a two step procedure. In the first step the polymer is saturated with a non-reactive gas at fairly elevated pressures. Upon saturation, the polymer is removed from the pressure reactor in order to produce a supersaturated sample. This supersaturated polymer is then heated to a temperature near T_g, thus inducing nucleation and growth of gas bubbles resulting in a porous structure. Carbon dioxide or nitrogen are mostly used as blowing agents. The bubble growth is arrested by quenching the samples in water at room temperature[6].

* To whom correspondence should be addressed

The second technique for the preparation of a foam is termed emulsion derived foams[7]. In this strategy preformed domains of a liquid component are stabilized by surfactants in order to prevent macroscopic phase separation. An emulsion consists mainly of three different parts, the continuous or outer phase, the dispersed or inner phase and the surfactant. The surfactant is an amphilic moiety, which ensures the miscibility between the inner and the outer phase. As the volume fraction of the inner phase exceeds the highest density packaging of spheres (74%), the inner phase can no longer stay separated, resulting in a co-continuous morphology. This type of morphology is known as high internal phase emulsion[8] or concentrated emulsion[9,10]. If the outer phase is a polymerizable monomer, a rigid matrix will form upon polymerization. A foam is obtained after removal of the inner phase, which is most often a low molecular weight liquid such as water. This principle allows the synthesis of organic as well as inorganic foams, offering a wide range of application. Emulsion derived foams are characterized by highly interconnected pores offering density values as low as $0.02\,g\,cm^{-3}$ and a narrow size distribution resulting from a thermodynamically stable system.

In contrast to the highly interconnected pores resulting from the above techniques, closed pores can also be obtained by microemulsion polymerization, if the initial volume fraction of the dispersed phase is lower than 30%. Recently two systems have been reported, where the polymerization of the continuous phase and the subsequent removal of the liquid dispersed phase resulted in the formation of porous thermoplastic materials, such as PS[11] or PMMA[12]. However, in this case the pore size was observed to be several micrometers, and not the expected nanofoam consistent with the microemulsion size (10–100 nm).

Amazingly small and well organized porous structures can be obtained from the self-assembly of tailor-made copolymers. Hedrick and coworkers[13–15] have explored a general methodology, enabling for the synthesis of mesoporous polyimides with a well controlled porosity, resulting from the self-assembly of triblock copolymers consisting of a thermally labile and thermally stable block. Thermal degradation of the thermally labile out phase leads to a well controlled porosity. Small angle X-ray scattering showed closed pores with sizes of about 5–20 nm, depending on the length of the thermally labile block. The generation of such a mesoporous structure results in a significant lowering of density and dielectric constant, thus offering great potential for applications in microelectronics.

The third technique to porous structures involves an initial phase separation followed by a solidification to fix the morpholgy and finally the removal of the minor separated phase. If a polymer-solvent film is immersed into a non-solvent precipitiation will occur, in accordance with this mechanism, leading to the formation of a polymer rich and solvent rich phase. This technique is largely applied to produce membranes, known as phase inversion membranes[16]. The membrane morphology can be varied from a sponge-like structure to a finger-like structure, depending on the processing parameters[17,18].

Another well known method is the preparation of macroporous polystyrene beads for chromatography. Recent progress in morphology control has resulted in better control of pore size and pore size distribution[19,20]. In this approach the inner phase consists of a mixture containing the reactive styrene and divinylbenzene monomers along with an unreactive substance, the porogen. After polymerization, the soluble fraction is washed out, leaving behind macroporous beads with pore sizes between 50 and 1000 nm depending on the polymerization temperature.

Phase separation followed by solidification can also be achieved by a temperature quench. Porous PS foams with densities as low as $0.02–0.2\,g\,cm^{-3}$ are produced by phase separation starting from a PS–cyclohexane system[21,22]. The phase diagram of this particular system is well known and exhibits an upper critical solution temperature. Above the critical solution temperature the cyclohexane and polystyrene are miscible. A phase separation is initiated by cooling below the binodal or spinodal line, thus resulting in a two phase morphology. Later this method has been termed 'thermally induced phase separation' (TIPS)[23,24]. Controlling the morphology requires a detailed knowledge of the phase diagram, as well as the thermodynamics and kinetics of the phase separation mechanism. Depending on the quenching temperature, the phase separation proceeds either via nucleation and growth or via spinodal decomposition, resulting in different morphologies. Thus the pore size can be varied from less than 1 μm up to around 100 μm. The low volume fraction of the polymeric phase leads to a highly interconnected, porous structure. This technique allows only for the preparation of films with less than 1 mm in thickness, which can be used as membranes. Furthermore this method is limited to thermoplastic polymers since it requires sufficient mobility of the polymeric phase below its T_g.

Very similar to a temperature quench, the pressure can be changed, leading to phase separation and solidification and hence to a porous structure. Currently several groups are investigating the feasibility to produce porous polymers by using supercritical carbon dioxide[25,26]. If the gas and the polymer are subjected to supercritical conditions, they become miscible. Phase separation resulting in a porous structure is envisaged by carrying out a rapid pressure quench. The concept of copolymeric surfactants is applied to stabilize the gas phase and hence to achieve a better control of the pore size distribution.

Our objective is to establish a general strategy to synthesize macroporous thermosets with pore sizes in the micrometre range. The strategy we sought to employ relates to the third group by generating a two phase morphology via a phase separation process resulting from a 'chemical quench'. Therefore this technique may be termed 'chemically induced phase separation' (CIPS)[27]. In fact, this approach is commonly used for the generation of a phase separated morphology in toughened epoxies with an elastomer or a thermoplastic as the dispersed domain[28–31]. The domain size of the second phase varies typically between 0.5 and 10 μm. Even when toughening with second phase particles is well established, there still exists a controversial discussion concerning the micromechanisms responsible for toughening, especially the importance of cavitation[32–37]. Cavitation is similar to the generation of well dispersed voids. Very recently Kinloch and Guild[38] calculated the stress distribution in the vicinity of dispersed holes in an epoxy matrix based on a finite element model. They

concluded that well-dispersed voids should significantly toughen epoxies. These theoretical predictions are in good agreement with previous experimental results. Pearson[39,40] and Kinloch[41] created pseudo-porous epoxies by using either hollow latex spheres or unreactive rubber monomers as the dispersed phase. Based on these model systems, they demonstrated the ability of voids to toughen epoxies in the same manner and same magnitude as rubber particles. Nevertheless they did not succeed in creating a real porous morphology in perfect agreement with the analytical model. It is the purpose of this paper to present a general approach for the preparation of macroporous thermosets with homogeneously distributed pores and a narrow size distribution in the μm-range, without any other alteration of the matrix.

In our concept, the initial system consists of the polymeric precursor and a low molecular weight liquid having a low boiling point, which will form a second phase upon the formation of a crosslinked network. The judicious choice of the organic liquid is critical as the low molecular weight liquid must be a good solvent for the reactive monomers yet poor for the cured network. After phase separation, the liquid phase should be removed by drying above T_g thus leaving a porous structure.

EXPERIMENTAL

Materials

Diglycidylether of bisphenol A (DGEBPA) (DER332 from DOW), 2,2′-bis(4-amino-cyclohexyl)propane (HY2954 from Ciba-Geigy), hexane and cyclohexane (from Fluka) were used as received.

Procedure

A general procedure for the preparation and curing is given by the following example for a sample with 10 wt% hexane.

4.21 g of epoxy and 1.5 g of diamine, giving a stochiometric ratio of 2 : 1, were mixed together with 0.963 ml of hexane under gentle stirring in a 20 ml flask. About 1.5 g of this clear solution was then transferred into a 5 mm diameter glass tube sealed at one end and placed in liquid nitrogen. After sealing the glass tube under an applied vacuum, the sample was homogenized by melting the hexane at room temperature. This resulted in a foam, which subsequently collapsed, forming a homogeneous, transparent solution. The sealed glass tube was then placed in a pre-heated sandbath at 40°C for 20 h in order to maintain a constant temperature and to avoid damage due to the explosion risk. The sample tube was then opened and the white solid epoxy–hexane sample was heated up to 200°C in a vacuum oven for 120 h in order to complete the network formation and to fully evaporate the hexane.

Characterization methods

The sample morphology was investigated by scanning electron microscopy (SEM) using a Cambridge S-100 operating at 10 kV. Therefore samples were fractured with a razor blade at room temperature and sputtered with gold using a Bio Rad SEM coating system E 5400. Image analysis was performed using the Optilab Pro2.6 software on an average of 4 SEM micrographs recorded with an acceleration voltage of 10 kV showing at least 150 pores. The glass transition temperature (T_g) was determined by dynamic mechanical analysis on a Rheometrics RSAII analyser operating in the compression mode with a constant frequency of 1 Hz on cylindrical samples, 5 mm in diameter and 10 mm in length, in the temperature range from 20 to 250°C. The maximum of the tan δ peak was taken as the T_g value. Densities were measured based on the Archimedes principle by using a Mettler AT261 balance equipped with the corresponding accessory. The time required for complete drying was determined by periodically measuring the residual weight loss of solvent from the samples using a Perkin–Elmer thermogravimetric analyser TGA7.

RESULTS AND DISCUSSION

The procedure to prepare macroporous epoxies via chemically induced phase separation is presented in *Scheme 1*. First the epoxy precursor, curing agent and low molecular weight liquid are mixed in the desired amount to give a homogeneous mixture. This one phase system is transferred into a glass tube and cooled by liquid nitrogen in order to freeze the solvent and arrest the exothermic curing reaction. Sealing the glass tube under the action of an applied vacuum leads to a closed system, thus allowing curing temperatures above the boiling point of the liquid without any solvent loss. Upon isothermally curing at the desired temperature, phase separation leads to opaque, solid samples, composed of the cross-linked resin and dispersed liquid domains. The formation of a porous morphology is achieved by heating above the infinite T_g (T_g^∞) of the fully cross-linked epoxy network allowing for evaporation of the low molecular weight liquid.

Analysis of the phase separation mechanism

The key to control the morphology of any type of two phase materials, prepared via a phase separation process, is the identification of the phase separation mechanism.

From a thermodynamic viewpoint, a phase separation is the result of a change in the free energy of the system. For a system composed of a polymer and solvent, the free energy of mixing, ΔG_m, had been derived independently by Flory and Huggins in the early 1940s based on the lattice model. Considering only weak interactions between both components, as well as random distribution of the two phases, their calculations led to the well-known Flory–Huggins equation[42].

$$\frac{\Delta G_m}{RT} = N_1 \log \phi_1 + N_2 \log \phi_2 + \chi_{12}\phi_1\phi_2(N_1 + xN_2) \quad (1)$$

where subscript 1 stands for the polymer and subscript 2 for the solvent, N_i represents the number of moles, ϕ_i the respective volume fractions, R the gas constant and T the absolute temperature. For a thermoset, the volume fraction of the cross-linked polymer depends on the extent of reaction. The interaction parameter χ_{12} depends itself on the temperature as well as on the volume fraction of the solvent[43]. The constant x is given by the relationship between the molar volumes of the polymer and solvent.

Regardless of the severe restrictions for the derivation of the Flory–Huggins equation, this theory has been successfully applied to explain the phase separation behaviour of rubber modified epoxies via reaction

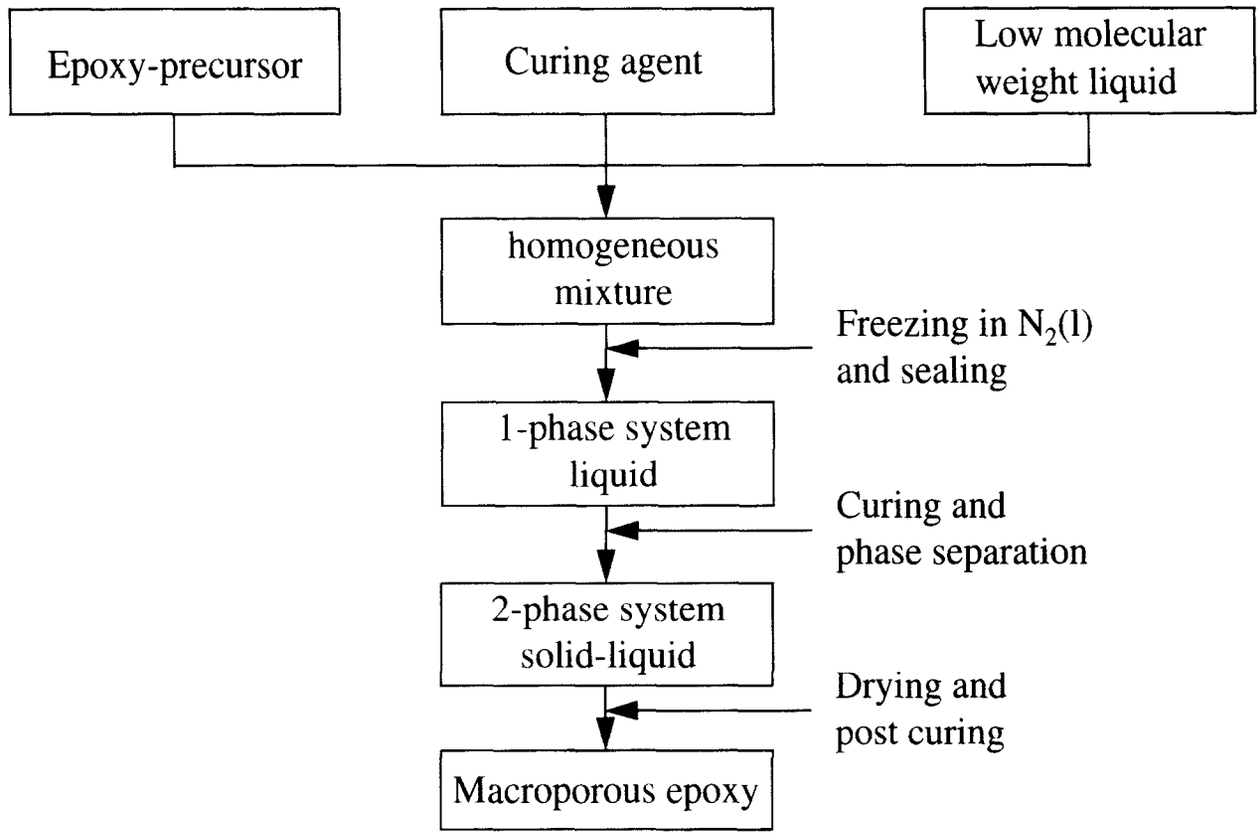

Scheme 1 Preparation method of macroporous epoxies via chemically induced phase separation (CIPS)

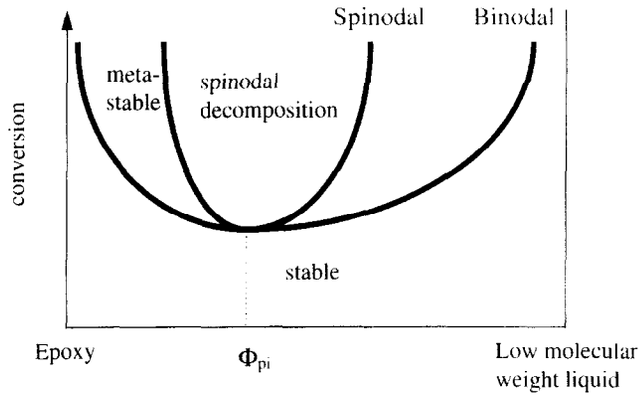

Figure 1 Principle phase diagram of chemically induced phase separation (CIPS)

induced phase separation[44], wherein the second phase is usually an oligomeric moiety containing polar groups. The free energy of mixing depends on the molecular weight of the polymeric phase and hence is a function of the extent of reaction. Schematic phase diagrams (*Figure 1*) can be derived from the free energy curves, based on the Flory–Huggins equation, expressed as a function of the reaction extent[45]. Such schematic phase diagrams are composed of three different regions and are very useful to explain the behaviour of our system. At low conversions, the polymer and solvent are miscible over the entire range corresponding to a one phase region. Entering the metastable region, that is enclosed between the binodal and spinodal curve, initiates the phase separation via a nucleation and growth mechanism. The binodal line results from the free energy curve by interconnecting all the points, where the two phases have the same chemical potential. Hence this represents the equilibrium curve. The curve that separates the metastable and spinodal region is called the spinodal line. The spinodal line results from the summation of inflexion points in the free energy curve. As the gradient of the free energy vs. the solvent concentration is negative between the inflexion points, separated domains are formed by the diffusion from the matrix to domains of high concentrations. Therefore this type of phase separation has been termed up-hill diffusion or spinodal decompositon[46,47].

The morphologies that are obtained via nucleation and growth can be quite different from those obtained by spinodal decomposition.

The energy balance of a system that phase separates via a nucleation and growth mechanism is governed by the energy required to enlarge the new surface and by the energy gain that results from the formation of a greater volume. Hence the second phase will take the shape that offers the best volume to surface ratio. Therefore the domains formed via nucleation and growth should ideally be spherical.

The morphology development upon spinodal decomposition proceeds through various stages[48]. In the early stage of decomposition a co-continuous structure develops. A two phase structure with dispersed domains is achieved only in the late stage of phase separation and the shapes of these domains are not uniform. In our strategy, using a system composed of a thermosetting polymer and a low molecular weight liquid, a co-continuous liquid phase, accompanied by a dramatic decrease in stiffness and strength, must be avoided. Thus spinodal decomposition should be avoided.

We are therefore looking for systems, where the phase

separation proceeds via a nucleation and growth mechanism, thus resulting in the formation of a closed cell structure, wherein the dispersed phase consists of a low molecular weight liquid and the matrix of a highly cross-linked polymer. Then the amount of solvent is limited by the phase inversion concentration, that is given by the interception of the binodal and spinodal line (Φ_{pi} in *Figure 1*). By this strategy, the final morphology is a result from the competing effects between the growth of the separated liquid domains and the continuous advancement in crosslinking.

The experimental identification of the phase separation mechanism is not trivial. Inoue and Yamanaka[49] investigated the phase separation of rubber in an epoxy matrix with light scattering measurements. Therefrom, they conclude a spinodal decomposition. Lee and Chen[50] examined a similar system with optical light microscopy and concluded a nucleation and growth mechanism. However, the later observations can also be consistent with a coalescence in the late stage of spinodal decomposition, as it is not possible to visualize nucleation with optical microscopy. It is not in the scope of this paper to investigate the phase separation mechanism experimentally. Nevertheless the phase separation process can be identified easily, only based on the schematic phase diagram, derived from the Flory–Huggins equation and presented in *Figure 1*, and a fundamental knowledge of the kinetics of this type of phase separation.

For the system diglycidylether of bisphenol A and 2,2′-bis(4-amino-cyclohexyl)propane, the desired phase separation is achieved, if hexane or cyclohexane are used as the low molecular weight liquid. Further discussion of the phase separation behaviour requires a more detailed regard to the schematic phase diagram, as presented in *Figure 4*. The critical amount for phase separation, ϕ_c, is given by the intercept of the binodal line and the conversion at gelation. Hence no phase separation occurs if gelation is reached before the metastable region is entered. If hexane is chosen as the selective solvent, the curing temperature is limited to 40°C to maintain homogeneous samples. Upon isothermally curing at 40°C, samples with concentrations of 5 wt% hexane or lower stay transparent and no sign of separated domains can be detected even with transmission electron microscopy. This corresponds to situation in *Figure 4*. Phase separation resulting in the formation of white, opaque samples is only observed at concentrations above 6 wt% hexane. Hence, ϕ_c (40°C) is found experimentally to be situated between 5 and 6 wt% hexane.

SEM micrographs of the opaque samples prepared with concentrations above ϕ_c, such as 6 and 7.5 wt% hexane are shown in *Figures 2a* and *b*. It can be clearly seen that the desired closed cell morphology including a narrow pore size distribution has been successfully achieved.

The fracture is influenced by the presence of voids leading to a fracture surface not representing a cut through the sample. Furthermore the voids may have been fractured at the centre or at the bottom or top. Hence, the domains seen with SEM on the fracture surface deviate from the true size of the voids. In addition the electron beam penetrates into the material and one does actually see holes in the bulk slightly below the real surface. These holes are likely to show the real radius but lead to an overestimation of the volume

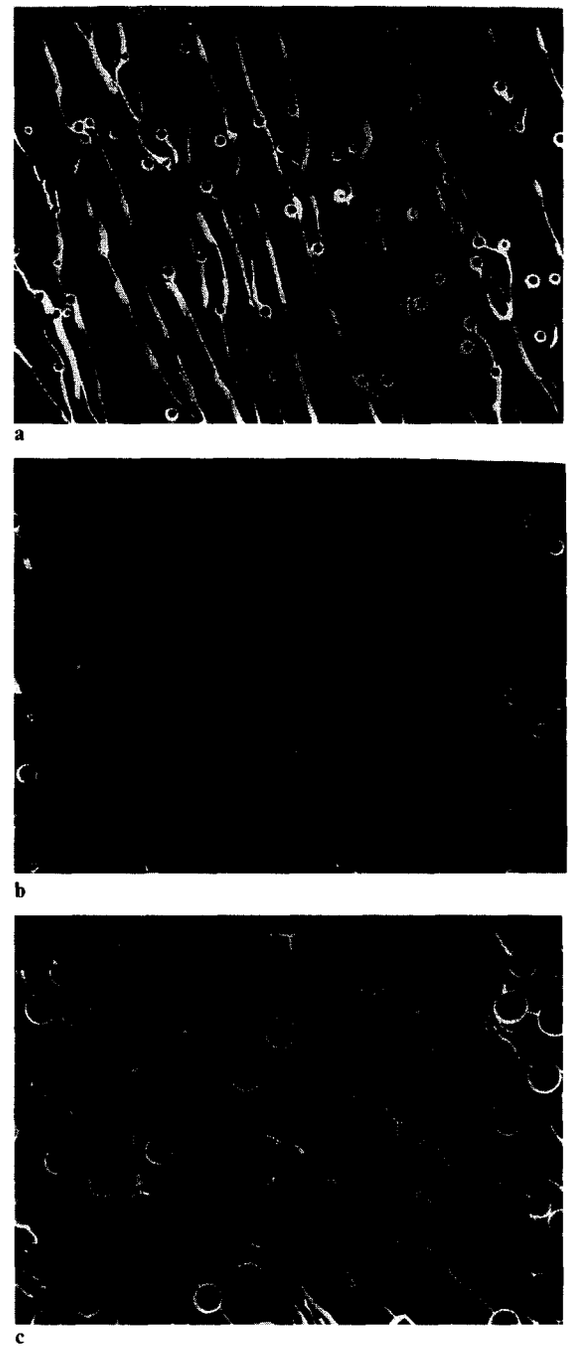

Figure 2 **(a)** SEM micrograph of macroporous epoxy prepared via CIPS with 6 wt% hexane cured at $T = 40°C$. **(b)** SEM micrograph of macroporous epoxy prepared via CIPS with 7.5 wt% hexane cured at $T = 40°C$. **(c)** SEM micrograph of macroporous epoxy prepared via CIPS with 10 wt% hexane cured at $T = 40°C$

fraction of voids from the SEM micrographs. However, as the acceleration voltage has been kept constant for all samples, SEM provides a good representation of both size and distribution, allowing us to compare different systems and conditions.

Scanning electron microscopy including image analysis were performed prior to and after the thermal removal of the hexane. These studies clearly indicate an increase in mean pore size, pore size distribution and volume fraction with increasing amount of hexane, once the critical concentration necessary for phase separation has been passed. These situations resulting in the formation of a narrow pore size distribution corresponding to lines B

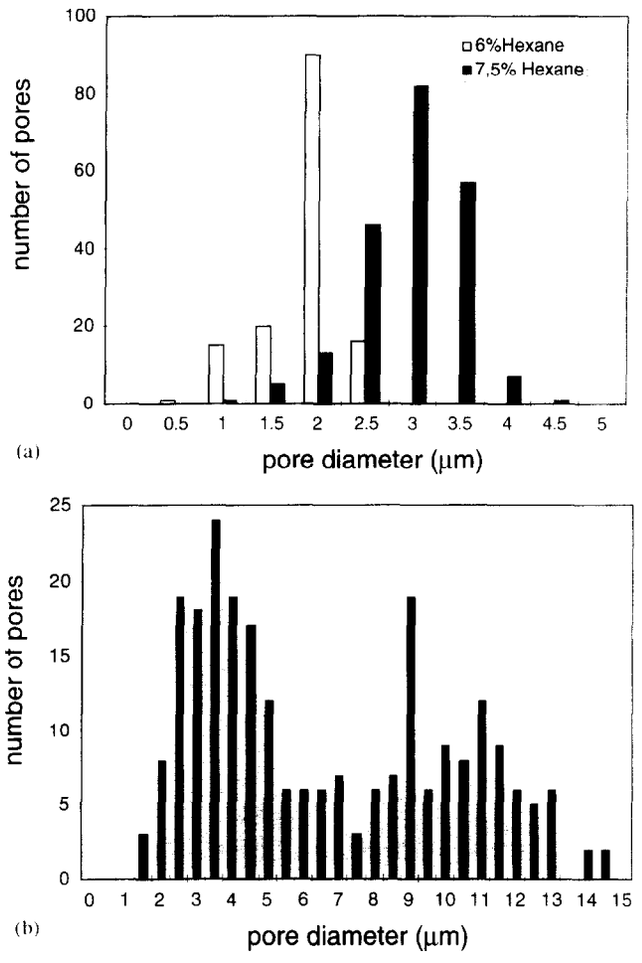

Figure 3 **(a)** Pore size distribution for macroporous epoxies prepared with 6 and 7.5 wt% of hexane cured at $T = 40°C$. **(b)** Pore size distribution for macroporous epoxies prepared with 10 wt% of hexane cured at $T = 40°C$

and C are represented in the schematic phase diagram (*Figure 4*). The pore size distributions calculated from image analysis of the sample with 6 and 7.5 wt% hexane are plotted in *Figure 3a*, clearly showing a narrow size distribution and an increase of pore size with increasing hexane concentration.

A further increase in the amount of solvent leads to the development of a bimodal pore size distribution, as observed with SEM (*Figure 2c*) as well as image analysis (*Figure 3b*) of a sample prepared with 10 wt% hexane. Such bimodal distribution has also been reported in rubber modified epoxies[51,52] prepared via phase separation. Regarding the kinetics of phase separation allows an explanation of the development of such a bimodal distribution and to identify the phase separation mechanism.

Supposing a homogeneous nucleation, the nucleation rate is given by[53]

$$\frac{dN}{dt} = N_0 D e^{-\frac{\Delta G_n}{RT}} \tag{2}$$

where N_0 represents the number of nuclei at the start of phase separation, ΔG_n is the activation energy for the creation of a nuclei, and R and T are the universal gas constant and absolute temperature respectively. In the case of a thermosetting material, the diffusion constant D is a complex function that depends on the temperature and the viscosity, which itself changes with the continuous advancement in cross-linking density and hence with time. The integration gives rise to an exponential decrease in the number of nuclei with time after the start of phase separation.

The growth rate, characterized by the change of the radius with time, is proportional to the driving force for the phase separation, given by the differences of the chemical composition of the second phase in the continuous phase at any time, ϕ_2^c, and its equilibrium composition given by the binodal line, ϕ_2^{eq}. The proportionality factor, given by the quotient of the diffusion constant D and the radius r, is called the mass transfer coefficient. ϕ_0 represents the initial solvent concentration. This is mathematically expressed by[54]

$$\frac{dr}{dt} = \frac{D(\phi_2^c - \phi_2^{eq})}{r(\phi_0 - \phi_2^{eq})} \tag{3}$$

As the growth rate is inversly proportional to the domain radius, smaller domains are able to grow faster than larger ones, thus giving rise to a narrow size distribution.

Based on equations (2) and (3), the development of a nearly monomodal or bimodal distribution can be qualitatively explained without the detailed knowledge of the real phase diagram nor the exact dependency of the diffusion constant as a function of time. The final morphology depends mainly on the extent of reaction at which the metastable region is entered, as discussed below.

For concentrations slightly above ϕ_c, the phase separation starts at high conversions (lines B and C in *Figure 4*), hence with an initial high viscosity. Even though the diffusion constant is low, the initially formed small domains grow fast [equation (2)]. After a certain period, the growth rate slows down to zero owing to two different contributions. First, as the composition approaches the equilibrium concentration, the driving force tends to approach zero and second, as gelation, accompanied by a dramatic increase in viscosity, is reached. This situation is responsible for the generation of a narrow size distribution at concentrations slightly above ϕ_c. The time evolution of the nucleation and growth rates responsible for the generation of a narrow pore size distribution are schematically shown in *Figure 5a*.

At higher concentrations of hexane, however, the

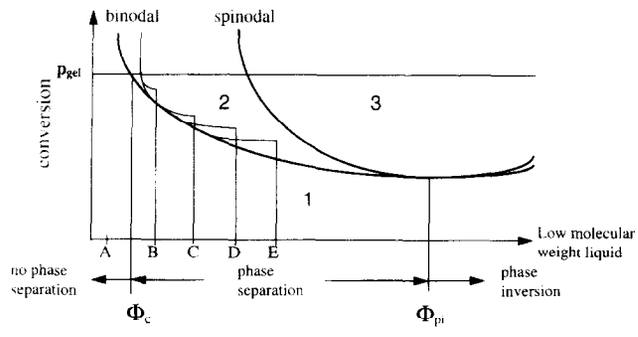

Figure 4 Schematic phase diagram for macroporous thermosets prepared via chemically induced phase separation (CIPS): 1, no phase separation; 2, phase separation via nucleation and growth; 3, phase separation via spinodal decomposition

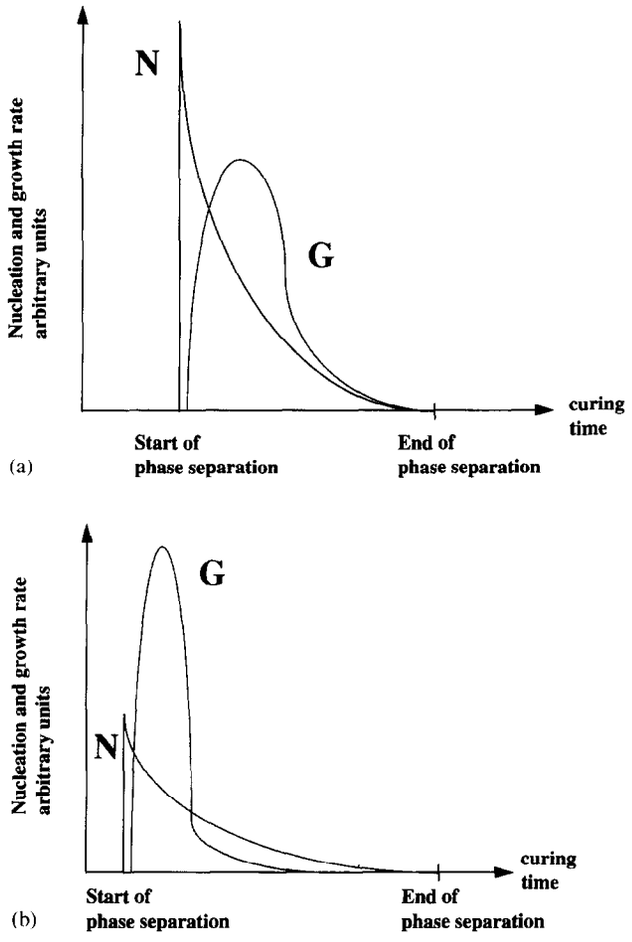

Figure 5 **(a)** High nucleation rate (N) and low growth rate (G) resulting in narrow size distribution. **(b)** Low nucleation rate (N) and high growth rate (G) resulting in bimodal size distribution

metastable region is entered at lower conversions, hence lower viscosity. Thus the diffusion constant is higher, leading to a very fast growth of the separated domains immediately after the start of the phase separation. This allows the system to reach the equilibrium concentration after a short period. As a consequence the driving force for the phase separation becomes nearly zero, and the growth rate is slowed down considerably well before gelation. At this time however, nucleation is still active, as shown in *Figure 5b*, representing the corresponding nucleation and growth rates. Only the small domains formed after this period are able to grow significantly, but their final size will be smaller than for the droplets formed in the early stage of phase separation. This finally leads to a bimodal distribution. This behaviour is schematically represented by lines D and E in *Figure 4*. Based on this model it can be concluded that the phase separation, resulting in a bimodal distribution, proceeds via nucleation and growth rather than via spinodal decomposition. The chemical quench at low curing temperatures allows a continuous and smooth transition from the stable to the metastable region and therefore favours the nucleation and growth mechanism. In contrast spinodal decomposition has been observed very often as a consequence of a temperature quench especially in systems where the exact phase diagram is not known in advance. Therefore the CIPS technique allows for the synthesis of macroporous thermosets with controlled morphology ranging from a narrow to a bimodal distribution.

Influence of chemical nature of phase separating liquid

In the previous section, we discussed the phase separation behaviour for the synthesis of macroporous epoxies by using hexane to form the dispersed phase. In the following, we will discuss the influence of several internal and external parameters, such as the chemical nature of the solvent, its concentration and the curing temperature on the morphology.

Experimentally, it is found that cyclohexane is also a candidate to give phase separation in the DGEBA–diaminocyclohexane system. The solubility parameters of hexane ($\delta_{hex} = 14.9$ $(J cm^{-3})^{1/2}$) and cyclohexane ($\delta_{chex} = 16.8$ $(J cm^{-3})^{1/2}$) are reported in literature[55]. The solubility parameter of the epoxy–cycloaliphatic diamine system can be calculated based on the molecular contributions as proposed by Hofytzer and van Krevelen[56]. Upon curing it increases from 18.3 $(J cm^{-3})^{1/2}$ for the non-reacted components to 20.4 $(J cm^{-3})^{1/2}$ for the crosslinked system. Even when the solubility parameter of hexane and cyclohexane does not vary significantly, a great difference in the phase separation behaviour is observed. Choosing an identical curing temperature of 40°C, phase separation resulting in the formation of white, opaque samples is observed at concentrations equal or above 14 wt% cyclohexane. This behaviour is not surprising. As the solubility parameter of cyclohexane is closer to that of the crosslinked epoxy, a higher amount of cyclohexane can be dissolved in the

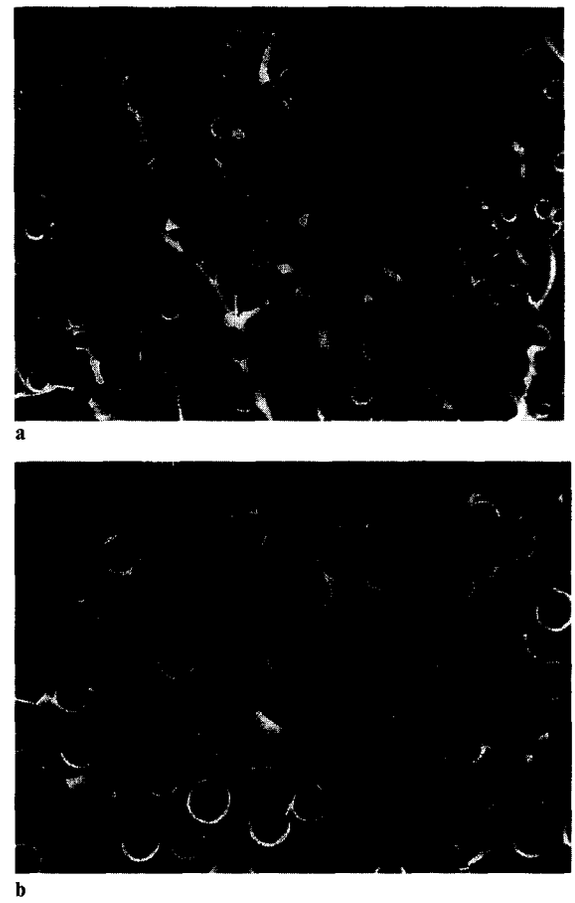

Figure 6 **(a)** SEM micrograph of macroporous epoxy prepared via CIPS with 15 wt% cyclohexane cured at $T = 40°C$. **(b)** SEM micrograph of macroporous epoxy prepared via CIPS with 20 wt% cyclohexane cured at $T = 40°C$

matrix. These experiments reveal that a change in solubility parameter of the solvent causes a decay in the critical amount of phase separation, ϕ_c, given by the intercept of the conversion at gelation and the binodal line. Currently, we are studying several systems to find a relationship between the difference of solubility parameter from solvent and matrix material and ϕ_c.

Influence of concentration of phase separating liquid

Regardless of the large difference in ϕ_c, the morphologies that are obtained by using either cyclohexane or hexane as the selective solvent are very similar at concentrations slightly above ϕ_c. *Figure 6* shows the SEM micrographs of samples cured isothermally at $T = 40°C$ with 15 and 20 wt% cyclohexane. It can be seen that the desired closed cell morphology, including a very narrow pore size distribution, is successfully achieved. The mean pore size as well as the pore size distribution increases with increasing amount of solvent as confirmed by image analysis from SEM. *Figure 7* shows the dependence of pore size and pore size distribution as a function of the cyclohexane concentration. In contrast to the hexane system, no bimodal distribution is detected up to the solubility limit of cyclohexane at 25 wt%. At higher concentrations much of the solvent is expelled, and these results are not considered for the study of the influence of concentration on the structure–property relationship.

In comparison to the results obtained for the samples prepared with hexane, it is concluded that the pore size and volume fraction do not depend on the initial concentration of the solvent, ϕ_0, but only on the difference between ϕ_0 and ϕ_c (*Figure 8*). Similar qualitative results are also reported for rubber modified epoxies prepared via reaction induced phase separation[57].

Dynamic scanning calorimetry (d.s.c.) measurements were also carried out in attempts to verify the generation of separated domains. Interestingly, an endothermic peak at around 7°C, corresponding to the melting point of cyclohexane, could only be detected at concentrations higher than 25 wt% cyclohexane. The appearance of such a melting peak is either linked to the formation of largely interconnected pores or pores overcoming a critical size necessary for crystallization. For this particular epoxy–cyclohexane system, d.s.c. is therefore not a useful tool to detect dispersed domains with diameters lower than 10 μm.

Influence of curing temperature

The influence of curing temperature and concentration of cyclohexane on the phase separation behaviour is summarized in *Figure 9*. It can be seen that the critical amount of phase separation, ϕ_c, can be lowered by decreasing the curing temperature.

Regarding this temperature dependence, we wanted to find out whether it is possible to lower the pore size by approaching the start of phase separation to the onset of gelation, that is widely regarded as the end of phase separation[58]. Thus we chose a constant cyclohexane concentration of 20 wt% and cured a series of samples isothermally at temperatures ranging from room temperature to 120°C. Thus phase separation occurs at curing temperatures at or below 104°C, and transparent samples are obtained by curing at temperatures above 105°C. *Figure 10* shows the SEM micrograph of the sample

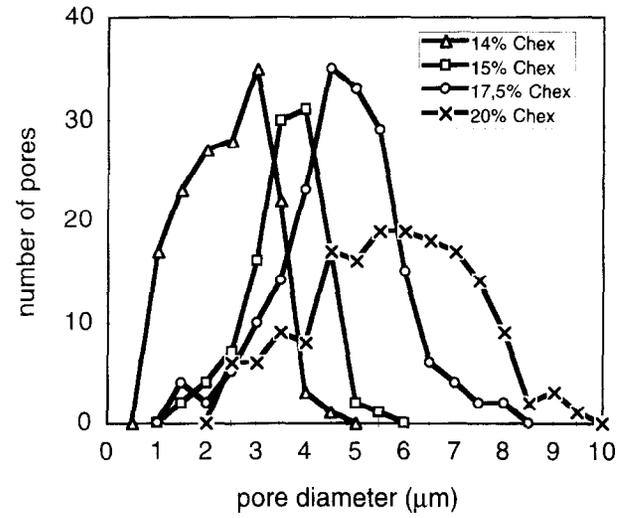

Figure 7 Pore size distributions of macroporous epoxies prepared via CIPS with cyclohexane cured at $T = 40°C$

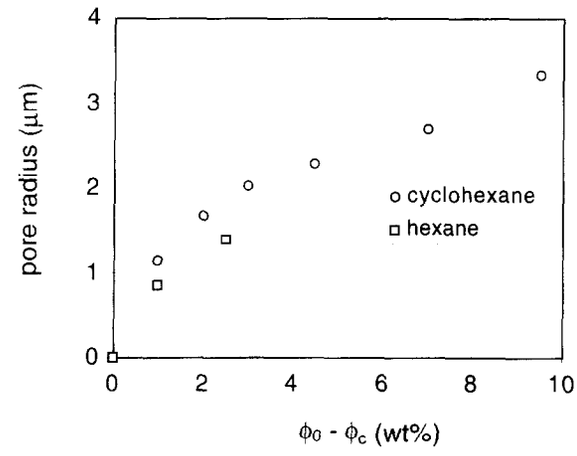

Figure 8 Pore size of macroporous epoxies prepared via CIPS. $\phi_0 - \phi_c$ difference between initial solvent concentration and critical solvent concentration

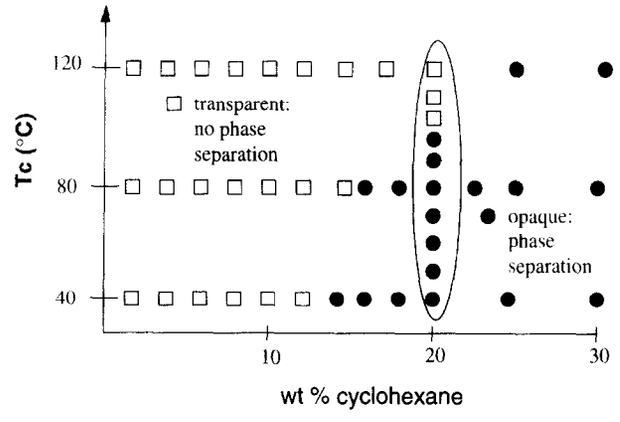

Figure 9 Phase separation behaviour of macroporous epoxies prepared via CIPS with cyclohexane

prepared at 104°C, exactly at the point where the start of phase separation should occur quasi-simultaneously with gelation. Pores with diameters ranging from around 1 to 6 μm appear. It seems, that the smallest domains are inhibited to grow further. Nevertheless, approaching the

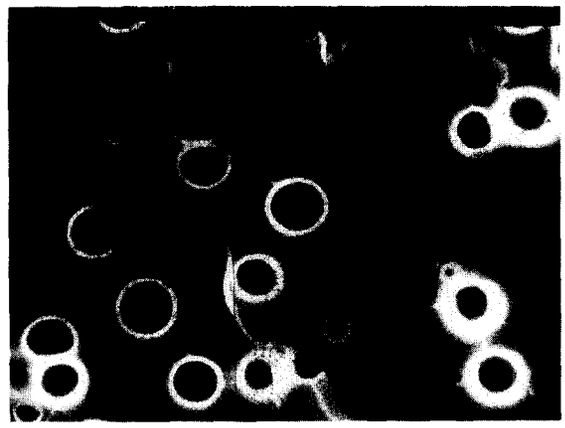

Figure 10 SEM micrograph of macroporous epoxy prepared with 20% cyclohexane cured at $T = 104°C$

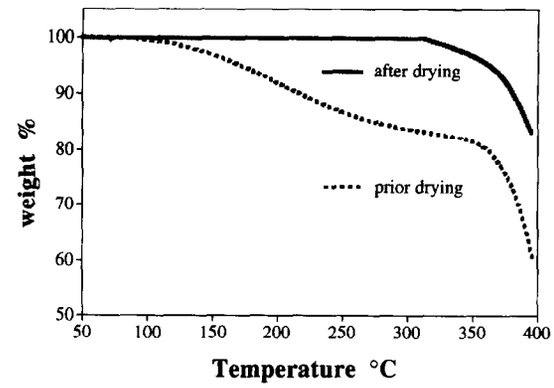

Figure 11 Weight loss of epoxies prepared via CIPS with 20 wt% cyclohexane prior and after the drying procedure

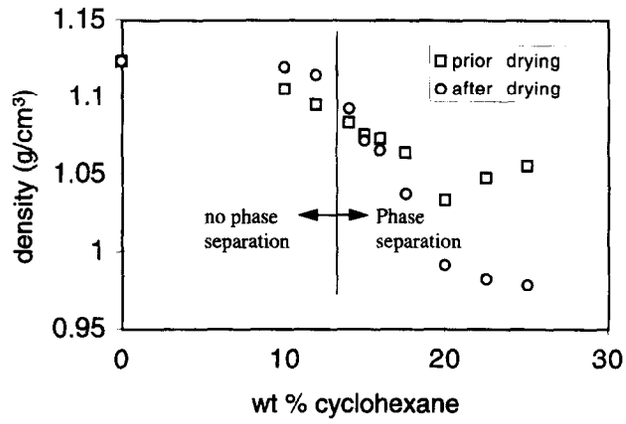

Figure 12 Density of cyclohexane modified epoxies prepared via CIPS prior to and after the drying procedure

phase separation line by either increasing the curing temperature for a constant concentration or raising the concentration for a given curing temperature does not allow for the preparation of pore diameters substantially less than 1 μm. In contrast, it is generally assumed, that the size of nuclei is typically less than 10 nm. There is still a controversal discussion, whether the end of phase separation is identical with the onset of gelation, or if a limited growth of the separated domains in the gelled state is still possible. Studying the phase separation behaviour in rubber modified epoxies, several authors have shown experimental evidence for the assumption, that phase separation is still possible after gelation[59–61]. Based on the above morphological observations, we conclude that, for our particular system, a time delay between the end of nucleation and the end of phase separation, allowing the nuclei to grow to around 1 μm, must exist. Therefore, we surmise that nucleation is stopped at gelation, whereas the liquid domains are able to grow further after gelation.

Development of porous structures

After phase separation, the creation of a porous morphology is achieved by treating the sample at a temperature well above the boiling point of the selective solvent and in the rubbery state of the fully cross-linked network, yet below the decomposition temperature of the network. Thus removal of the low molecular weight liquid was conduced by heating the samples above the T_g^∞ of the neat matrix ($T_g^\infty = 170°C$) at a temperature of 200°C for 120 h. The complete removal of the solvent was controlled with t.g.a. *Figure 11* shows the weight loss of samples prepared via CIPS with initially 20 wt% cyclohexane prior and after the drying procedure. The phase separation was achieved by curing at $T = 80°C$, thus 11 K above the boiling point of the cyclohexane. The t.g.a. measurement of the sample prior to drying clearly shows a weight loss of 20%, identical with the initial amount of solvent added, up to the onset of decomposition reactions at temperatures above 300°C. Thus no solvent loss occurs during the preparation of the phase separated samples. Furthermore, it can be concluded that temperatures above T_g are required to facilitate solvent evaporation. However, after the thermal drying, no weight loss is detected with t.g.a. below the decomposition temperature, hence the drying is completed. As the drying is performed via a diffusion process, the time for drying depends mainly on the drying temperature, the crosslink density of the network, the molecular structure of the liquid and the sample dimensions. Scanning electron microscopy including image analysis were performed prior to and after the thermal removal of the liquid phase. These investigations revealed no change in morphology, thus neither ripening or coarsening nor collapse of the dispersed domains occurred during the drying procedure.

The influence of the drying procedure on the density, both prior and after evaporation of the low molecular weight liquid, is plotted in *Figure 12* for samples cured with various amounts of cyclohexane. It can be clearly seen, that after drying, a considerable drop in density results from the formation of a porous morphology at concentrations above ϕ_c. However, no decrease in density is measured after the drying of transparent samples. In this case, the low molecular weight liquid is not involved in the formation of separated domains and after drying the fully cross-linked network is achieved by solvent evaporation from the matrix. Similar results were also obtained for macroporous epoxies prepared with hexane.

Prior to drying, the cyclohexane dissolved in the matrix has a plasticizing effect, thus lowering the T_g of the cross-linked product. This is shown in *Figure 13* where the T_g is plotted against the solvent concentration both prior and after thermal removal of cyclohexane.

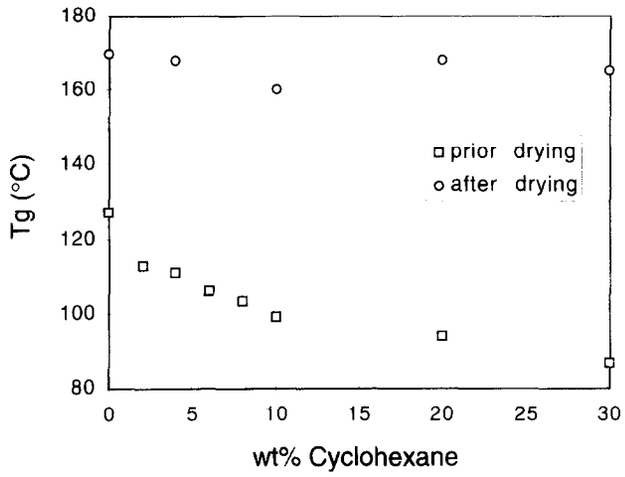

Figure 13 T_g of cyclohexane modified epoxies prepared via CIPS prior and after the drying procedure

Amazingly, no lowering of T_g is observed after the drying procedure, even at initial high amounts of cyclohexane. Thus, the final T_g of the matrix is independent of the amount of the selective solvent and T_g^∞ of the neat matrix can be reached upon drying. This shows that the solvent removal is achieved completely and a post-curing is realized simultaneously with the drying procedure. Chemically induced phase separation therefore allows for the synthesis of macroporous thermosets without lowering the dimensional stability or T_g of the fully cross-linked network. This is in contrast to rubber modified epoxies, where the network modifier fraction that is not involved in the phase separation, remains in the epoxy matrix after cure and hence leads to a decrease in T_g.

CONCLUSIONS

Macroporous epoxies with a narrow pore size distribution and a closed cell morphology are successfully synthesized by the chemically induced phase separation technique. The phase separation strongly depends on the chemical nature and amount of solvent, as well as on the curing temperature. A small change in solubility parameter can result in a large difference in the critical amount for phase separation, ϕ_c. The pore size and volume fraction depend mainly on the difference between the initial amount of solvent and ϕ_c. Pore size and volume fraction increase with the solvent concentration, once ϕ_c has been passed. Lowering the curing temperatures enables one to lower ϕ_c for the epoxy–cyclohexane system. Thermal removal of the solvent acts as a simultaneous post curing, hence the final T_g is independent of the initial amount of low molecular weight liquid. The chemically induced phase separation allows for the synthesis of macroporous epoxies with controlled morphology and considerable lower density without any other alteration of the cross-linked matrix.

ACKNOWLEDGEMENTS

Financial support from the Swiss National Fonds (No. 2100 039647.93/1) is gratefully acknowledged. The authors would like to thank Prof. H. H. Kausch, Mr R. Gensler, Dr D. Knauss and Dr L. Boogh for helpful discussions.

REFERENCES

1 Schaefer, D. W. *MRS Bull.* 1994, **19,** 14
2 Klempner, D. and Frisch, K. C. 'Handbook of Polymeric Foams and Foam Technology', Hanser, München, 1991
3 Shutov, F. 'Bicellular structure: A micro and macrocell concept for polymer foams', *ACS Nat. Meet. Abstract Book* 23–28 August 1992, Washington, **204,** Paper 15
4 Kumar, V. *Cell. Polym. Int. Conf.* 1993, **2,** 54
5 Ramesh, N. S., Rasmussen, D. H. and Campbell, G. A. *Polym. Eng. Sci.* 1994, **34,** 1698
6 Wing, G., Pasricha, A., Tuttle, M. and Kumar, V. *Polym. Eng. Sci.* 1995, **35,** 673
7 Even Jr., W. R. and Gregory, D. P. *MRS Bull.* 1994, **19,** 29
8 Lissant, K. J. and Mayhan, K. G. *J. Coll. Interf. Sci.* 1973, **43,** 201
9 Princen, H. M., Aronson, M. P. and Moser, J. C. *J. Coll. Interf. Sci.* 1980, **75,** 246
10 Ruckenstein, E. and Park, J. S. *Polymer* 1992, **33,** 405
11 Qutubuddin, S., Lin, C. S. and Tajuddin, Y. *Polymer* 1994, **35,** 4606
12 Gan, L. M., Chieng, T. H., Chew, C. H. and Ng, S. C. *Langmuir* 1994, **19,** 4022
13 Hedrick, J. L., Labadie, J., Russell, T., Wakharkar, V. and Hofer, D. *MRS Symp. Proc.* 1992, **274,** 37
14 Charlier, Y., Russell, T. P. and Hedrick, J. L. *MRS Symp. Proc.* 1994, **332,** 227
15 Hedrick, J. L., Russell, T. P., Labadie, J., Lucas, M. and Swanson, S. *Polymer* 1995, **36,** 2685
16 Loeb, S. and Sourirajan, S. *Adv. Chem. Ser.* 1962, **38,** 117
17 Strathmann, H. and Kock, K. *Desalination* 1977, **21,** 241
18 Fujita, S. M. and Soane, D. S. *Polym. Eng. Sci.* 1988, **28,** 341
19 Fréchet, J. M. J. *Makromol. Chem. Macromol. Symp.* 1993, **70/71,** 289
20 Svec, F. and Fréchet, J. M. J. *Macromolecules* 1995, **28,** 7580
21 Aubert, J. H. and Clough, R. L. *Polymer* 1985, **26,** 2047
22 Lal, J. and Bansil, R. *Macromolecules* 1991, **24,** 290
23 Song, S. W. and Torkelson, J. M. *Macromolecules* 1994, **27,** 6389
24 Song, S. W. and Torkelson, J. M. *Polym. Prepr.* 1993, **34,** 496
25 Desimone, J. M., Maury, E. E., Menceloglu, Y. Z., McClain, J. B., Romack, T. J. and Combes, J. R. *Science* 1994, **265,** 356
26 Goel, S. K. and Beckman, E. J. *Polym. Eng. Sci.* 1994, **34,** 1137
27 Pascault, J. P. *Macromol. Symp.* 1995, **93,** 43
28 Riew, C. K. and Gillham, J. K. 'Rubber-Modified Thermoset Resins', *Adv. Chem. Ser.* 1984, **208**
29 Riew, C. K. 'Rubber Toughened Plastics', *Adv. Chem. Ser.* 1989, **222**
30 Riew, C. K. and Kinloch, A. J. 'Toughened Plastics', *Adv. Chem. Ser.* 1992, **233**
31 Collyer, A. A. 'Rubber Toughened Engineering Plastics', Chapman & Hall, 1994
32 Sultan, J. N. and McGarry, F. J. *Polym. Eng. Sci.* 1973, **13,** 29
33 Sue, H. J. *J. Mater. Sci.* 1992, **27,** 3098
34 Bagheri, R. and Pearson, R. A. *Int. SAMPE Tech. Conf.* 1993, **25,** 25
35 Huang, Y. and Kinloch, A. J. *J. Mater. Sci. Lett.* 1992, **11,** 484
36 Lazzeri, A. and Bucknall, C. B. *J. Mater. Sci.* 1993, **28,** 6799
37 Dompas, D. and Groenickx, G. *Polymer* 1994, **35,** 4743
38 Guild, F. J. and Kinloch, A. J. *J. Mater. Sci.* 1995, **11,** 1689
39 Pearson, R. A. *Int. Conf. on Deformation, Yield and Fracture* 1994 **9,** P106/1–4
40 Bagheri, R. and Pearson, R. A. *Polymer* 1995, **36,** 4883
41 Huang, Y. and Kinloch, A. J. *Polymer* 1992, **33,** 1330
42 Champetier, G., Buvet, R., Néel, J. and Sigwalt, P. 'Chimie macromoléculaire', Hermann, Paris, 1972
43 Kumar, S., Taylor, J., Denenedetti, S. and Graessley, W. *Polym. Mater. Sci. Eng.* 1994, **71,** 358
44 Vazquez, A., Rojas, A. J., Adabbo, H. E., Borrajo, J. and Williams, R. J. J. *Polymer 1987,* **28,** 1156
45 Williams, R. J. J., Borrajo, J., Adabbo, H. E., Rojas, A. J. *Adv. Chem. Ser.* 1984, **208,** 195

46 Binder, K. in 'Materials Science and Technolgy' (Ed. P. Haasen), Vol. 5, VCH, Weinheim, 1991, pp. 405–472
47 Vollertsen, F. and Vogler, S. 'Werkstoffeigenschaften und Mikrostruktur', Hanser, München, 1989, pp. 197–200
48 Inoue, T. *Prog. Polym. Sci.* 1995, **20,** 119
49 Yamanaka, K. and Inoue, T. *J. Mater. Sci.* 1990, **25,** 241
50 Chen, J. P. and Lee, Y. D. *Polymer* 1995, **36,** 55
51 Kim, S. C., Ko, M. B. and Jo, W. H. *Polymer* 1995, **36,** 2189
52 Kinloch, A. J. and Hunston, D. L. *J. Mater. Sci. Lett.* 1986, **5,** 1207
53 Wagner, R. and Kampmann, R. in 'Materials Science and Technolgy' (Ed. P. Haasen), Vol. 5, VCH, Weinheim, 1991, pp. 243–247
54 Wagner, R. and Kampmann, R. in 'Materials Science and Technolgy' (Ed. P. Haasen), Vol. 5, VCH, Weinheim, 1991, pp. 253–254
55 Brandrup, J. and Immergut, E. H. 'Polymer Handbook', Wiley, New York, 1989
56 Van Krevelen, D. W., Hoftyzer, P. J. 'Properties of Polymers', Elsevier, New York, 1976
57 Verchere, D., Sautereau, H., Pascault, J. P., Riccardi, S. M., Moschiar, S. M. and Williams, R. J. J. *J. Appl. Polym. Sci.* 1991, **42,** 701
58 Manzione, L. T. and Gillham, J. K. *J. Appl. Polym. Sci.* 1981, **26,** 889
59 Chan, L. C., Gillham, J. K., Kinloch, A. J. and Shaw, S. J. *Adv. Chem. Ser.* 1984, **208,** 235
60 Kim, D. S. and Kim, S. C. *Polym. Adv. Techn.* 1990, **1,** 211
61 Riccardi, C. C., Borrajo, J. and Williams, R. J. J. *Polymer* 1994, **35,** 5541